



Cite this: *Chem. Commun.*, 2020, 56, 14071

Received 6th August 2020,
Accepted 8th September 2020

DOI: 10.1039/d0cc05365a

rsc.li/chemcomm

[LSi(η^2 -P₄)] (L = CH[C(Me)N(Dipp)][C(CH₂)N(Dipp)], Dipp = 2,6-diisopropylphenyl) forms well-defined 1 : 1 and 2 : 1 complexes with N-heterocyclic carbene nickel fragments. The cluster compound [(Dipp)Ni₂P₈(SiL)₂] (IDipp = 1,3-bis(2,6-diisopropylphenyl)imidazolin-2-ylidene) is selectively formed by thermolysis of the complex [(IDipp)-Ni(μ - $\eta^{2,2}$ -P₄)SiL].

Nickel phosphides are of interest in material science and industry due to their favourable magnetic and catalytic properties¹ and their potential in hydrogen evolution reactions (HER),² water splitting,³ hydrodenitrogenation and hydrodesulfuration reactions.^{4,5} Doping nickel phosphides with different transition metal elements is a common approach to modify their electro- and photocatalytic activity.⁶ Including main group elements, such as sulphur, has been shown to improve the catalytic activity of nickel phosphides in HER.⁷ Although promising, the synthesis of such metal phosphides remains challenging^{5,8} and contemporary methods require sensitive and toxic phosphine precursors (e.g. P(SiMe₃)₃), special additives (e.g. tri-*n*-octylphosphine, oleylamine) and high temperatures.^{9–11} A possible alternative is the mild thermolysis of carefully designed transition metal polyphosphido complexes,¹² which can be accessed by the direct activation of white phosphorus (P₄). The use of nickel(0) complexes already dates back to 1979, when Sacconi and co-workers reported the synthesis of a monohapto P₄ complex [(κ^3 -P₄P₃NP₃)Ni(η^1 -P₄)] [(NP₃ = tris(2-diphenylphosphinoethyl)amine)].¹³ Since then, several other groups have shown that Ni⁰ sources are suitable reagents for the targeted synthesis of nickel polyphosphido compounds.^{10,14–17} Le Floch and Mézailles prepared Ni₂P nanoparticles directly by reacting [Ni(cod)₂] (cod = 1,4-cyclooctadiene) with P₄ in the presence of TOPO (tri-*n*-octylphosphine oxide)

An unusual Ni₂Si₂P₈ cluster formed by complexation and thermolysis†

Christoph G. P. Ziegler,^a Clemens Taube,^b John A. Kelly,^a Gabriele Hierlmeier,^a Maria Uttendorfer,^a Jan J. Weigand^{b*} and Robert Wolf^{a*}

(Fig. 1, A)¹⁰ and Radius and co-workers accessed the P₂ complex [Ni(ImiPr₂)₂](μ - $\eta^{2,2}$ -P₂) (Fig. 1, B, ImiPr₂ = 1,3-bis(iso-propyl)imidazolin-2-ylidene).¹⁶ More recently, our group described the aggregation of P₄ using (NHC)Ni complexes leading to novel di- and trinuclear complexes (see e.g. Fig. 1, C).¹⁷

Molecular main-group doped nickel phosphide complexes were reported by Driess in 2009 (Fig. 1, D).¹⁸ This type of complex is obtained from [LSi(η^2 -P₄)]¹⁹ (L = CH[C(Me)N(Dipp)][C(CH₂)N(Dipp)]) and [(L'Ni)₂·toluene] (L' = CH[CMeN(Dipp)]₂) and [(L''Ni)₂·toluene] (L'' = CH[CMeN(2,6-Et₂C₆H₃)]₂).¹⁸ The molecular structures of these complexes feature an intact SiP₄ unit coordinating to the Ni^I centre.

We reasoned that reactions with a more strongly reducing Ni⁰ precursor could lead to P–P bond cleavage and subsequent

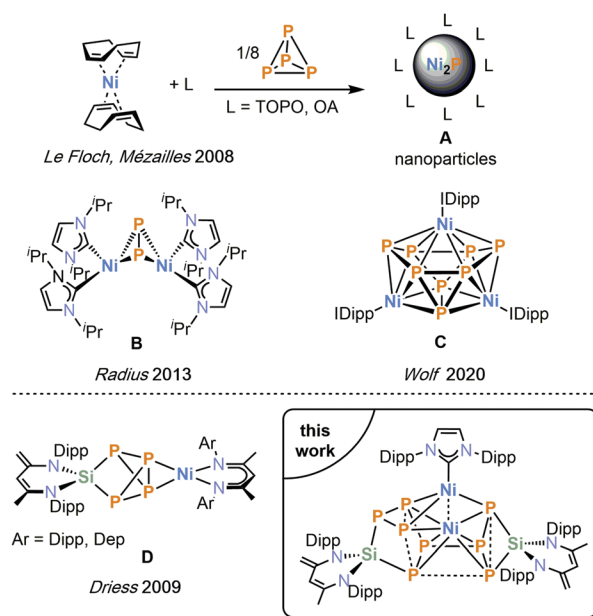


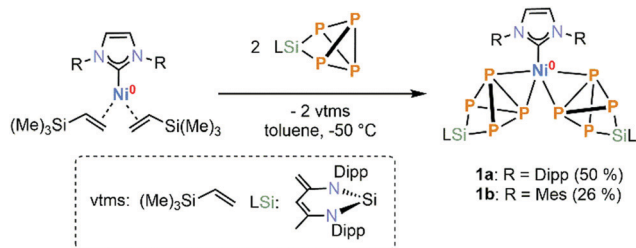
Fig. 1 Examples of P₄ activation by Ni⁰ precursors (top); heterodinuclear silicon–nickel polyphosphido complexes (bottom); Dipp = 2,6-diisopropylphenyl, Dep = 2,6-Et₂C₆H₃.

^a University of Regensburg, Institute of Inorganic Chemistry, 93040 Regensburg, Germany. E-mail: robert.wolf@ur.de

^b TU Dresden, Faculty of Chemistry and Food Chemistry, 01062 Dresden, Germany. E-mail: jan.weigand@tu-dresden.de

† Electronic supplementary information (ESI) available. CCDC 2009284–2009287. For ESI and crystallographic data in CIF or other electronic format see DOI: 10.1039/d0cc05365a





Scheme 1 Synthesis of $[(\text{NHC})\text{Ni}(\mu\text{-}\eta^2\text{-P}_4)\text{SiL}_2]$ [$\text{NHC} = \text{IDipp}$ (**1a**), $\text{NHC} = \text{IMes}$ (**1b**)].

aggregation of the resulting intermediates. Herein, we report the preparation of $(\text{NHC})\text{Ni}^0$ complexes with the tetraphosphasilatricyclopentane $[\text{LSi}(\eta^2\text{-P}_4)]$. Mild thermolysis of one of the complexes affords an unusual $\text{Ni}_2\text{Si}_2\text{P}_8$ cluster by the nickel-mediated dimerization of two $[\text{LSi}(\eta^2\text{-P}_4)]$ units.

Vinyltrimethylsilane complexes $[(\text{NHC})\text{Ni}(\eta^2\text{-vtms})_2]$ ($\text{NHC} = \text{IDipp}$, IMes , $\text{vtms} = \text{Me}_3\text{SiCH=CH}_2$) were selected as well-proven “ $(\text{NHC})\text{Ni}^0$ ” equivalents and reacted with $[\text{LSi}(\eta^2\text{-P}_4)]$ in a 1 : 1 and 1 : 2 stoichiometry in toluene at -50°C .^{19,20} Using two equivalents of $[\text{LSi}(\eta^2\text{-P}_4)]$, $[(\text{NHC})\text{Ni}(\mu\text{-}\eta^2\text{-P}_4)\text{SiL}_2]$ **1a** ($\text{NHC} = \text{IDipp}$) and **1b** ($\text{NHC} = \text{IMes}$) are isolated as red powders in 50% and 26% yield, respectively (Scheme 1). A single crystal X-ray diffraction (XRD) study revealed that both compounds are isostructural and therefore only **1a** will be discussed here. The molecular structure shows two $[\text{LSi}(\eta^2\text{-P}_4)]$ ligands side-on coordinated to the bridging $[(\text{IDipp})\text{Ni}]$ unit. The P–P bond distances of the coordinated P atoms (P3–P4 2.2686(6), P7–P8 2.4749(7) Å) are considerably longer than the corresponding P–P bond length in $[\text{LSi}(\eta^2\text{-P}_4)]$ (2.159(2) Å), although similar to complex **D** (2.351(3) Å).^{18,19} This might be explained by a significant back-donation of electron density from the Ni^0 centre. The Ni–P distances (av. 2.2744 Å) in **1a** lie in a similar range to those of **D** (av. 2.266 Å) (Fig. 2).¹⁸

The $^{31}\text{P}\{^1\text{H}\}$ NMR spectra of **1a** (Fig. S5, ESI†) shows two very broad resonances at $\delta = -234.3$ ppm and 190.6 ppm with an integral ratio of 1 : 1, which do not resolve at differing temperatures, suggesting a fluxional behaviour in solution (Fig. S7 and S8, ESI†). Complex **1b** shows comparatively sharper multiplets at $\delta = -236.4$ ppm and 194.2 ppm in the $^{31}\text{P}\{^1\text{H}\}$ NMR spectrum (Fig. S11, S13 and S14, ESI†). Despite the broad resonances observed in the ^{31}P NMR spectra, both **1a** and **1b** give rise to well-resolved ^1H NMR spectra (Fig. S3 and S9, ESI†), which indicate a symmetric structure. The ^{29}Si NMR spectrum of **1a** reveals a very broad signal at $\delta = -50.5$ ppm ($\nu_{1/2} = 90$ Hz), whereas **1b** displays a broad pseudo-triplet resonance at $\delta = -51.1$ ppm which is slightly shifted to higher field compared to the starting material $[\text{LSi}(\eta^2\text{-P}_4)]$ ($\delta = -40.4$ ppm).¹⁹

The reaction with equimolar amounts of $[(\text{IDipp})\text{Ni}(\eta^2\text{-vtms})_2]$ and $[\text{LSi}(\eta^2\text{-P}_4)]$ in toluene at room temperature results in the selective formation of a new species $[(\text{IDipp})\text{Ni}(\mu\text{-}\eta^2\text{-P}_4)\text{SiL}]$ (**2**). After filtration and recrystallisation from *n*-hexane, **2** was isolated as red crystalline blocks (Scheme 2). The solid-state structure of **2** reveals a heterodinuclear $[\text{Si}(\mu\text{-}\eta^2\text{-P}_4)\text{Ni}]$ core highly reminiscent of complex **D** (see the ESI† for full crystallographic data, NMR

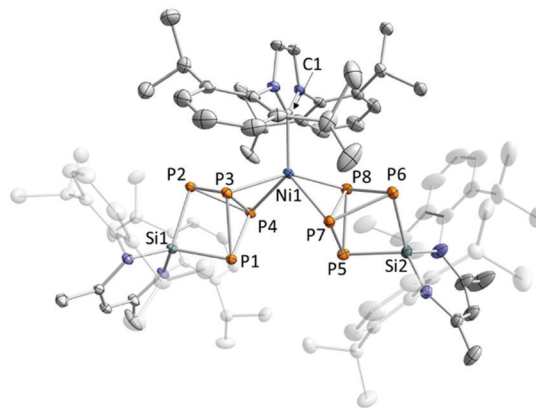
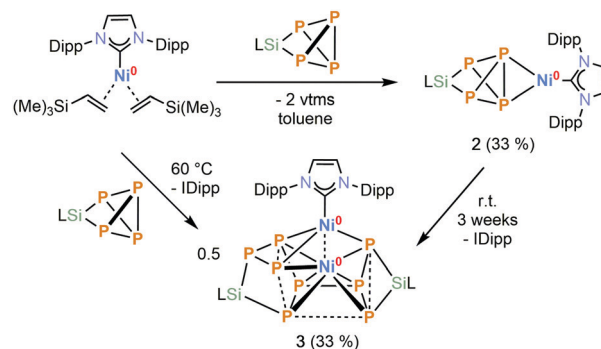


Fig. 2 Solid-state molecular structure of **1a**. Hydrogen atoms and solvate molecules are omitted for clarity; thermal ellipsoids are drawn at the 40% probability level; selected bond lengths [Å] for **1a**: P1–P3 2.2651(6), P1–P4 2.2511(7), P2–P3 2.2565(7), P2–P4 2.2724(7), P3–P4 2.2686(6), Si1–P1 2.2512(8), Si1–P2 2.2422(7), Ni1–P3 2.2923(8), Ni1–P4 2.2674(8), P5–P7 2.2451(6), P5–P8 2.2603(7), P6–P7 2.2714(9), P6–P8 2.2607(7), P7–P8 2.4749(7), Si2–P5 2.2475(9), Si2–P6 2.2455(6), Ni1–P7 2.2657(6), Ni1–P8 2.2847(7), Ni1–C1 1.9761(16); bond distances and angles of derivatives **1b** are presented in the ESI† (see Fig. S26).



Scheme 2 Synthesis of $[(\text{IDipp})\text{Ni}(\mu\text{-}\eta^2\text{-P}_4)\text{SiL}]$ (**2**) and $[(\text{IDipp})\text{NiP}_8(\text{SiL})_2]$ (**3**).

and bond analysis).¹⁸ When conducted with the less sterically demanding $[(\text{IMes})\text{Ni}(\eta^2\text{-vtms})_2]$ the exclusive formation of **1b** was observed.

Compound **2** slowly decomposes in solution and over the course of three weeks gives rise to a $^{31}\text{P}\{^1\text{H}\}$ NMR spectrum with two new ABCDEMSX spin systems, which are assigned to $[(\text{IDipp})\text{Ni}_2\text{P}_8(\text{SiL})_2]$ (**3**, *vide infra*). The clean formation of **3** can also be achieved by heating the reaction of $[(\text{IDipp})\text{Ni}(\eta^2\text{-vtms})_2]$ and $[\text{LSi}(\eta^2\text{-P}_4)]$ to 60°C , circumventing the isolation of **2**. Significant amounts of by-product IDipp were removed *via* sublimation (95°C and 1×10^{-5} mbar). Subsequent recrystallization from toluene layered with *n*-hexane afforded compound **3** as brown crystals in a 33% yield.

The structure of **3** shows an unusual asymmetrical $\text{Ni}_2\text{Si}_2\text{P}_8$ cluster with strongly varying P–P distances (range: 2.1702(8)–3.4219(8) Å). The phosphorus atoms P1, P3, P8, and P6 are aligned in a plane (torsion angle $\angle 1.8^\circ$) and coordinated by the central Ni1 atom. This plane is fused to a P_3 ring (P2, P4 and P5) with one



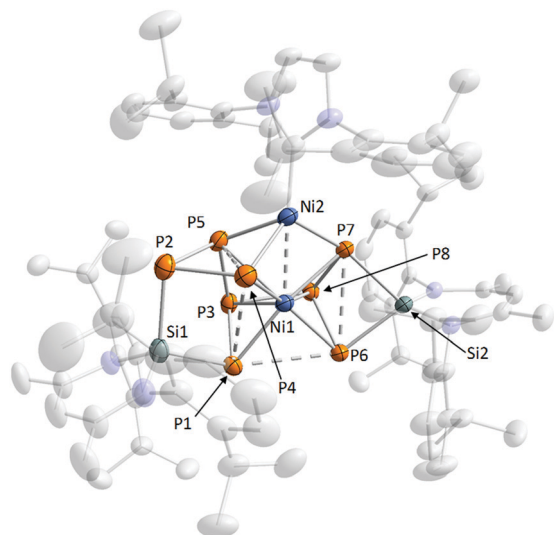


Fig. 3 Solid-state molecular structure of **3**. Hydrogen atoms and disorder are omitted for clarity; thermal ellipsoids are drawn at the 40% probability level; selected bond distances [Å] and angles [°] for **3**: P1–P3 2.1702(8), P1–P4 3.4219(8), P1–P6 3.0176(7), P2–P4 2.2160(9), P2–P5 2.1704(10), P4–P5 2.5499(9), P3–P8 2.4018(7), P6–P7 2.1946(7), P7–P8 2.3083(7), Si1–P1 2.2539(8), Si1–P2 2.2832(11), Si2–P6 2.2265(7), Si2–P7 2.2709(7), Ni1–Ni2 2.4126(4), Ni1–P1 2.2717(6), Ni1–P3 2.4280(6), Ni1–P6 2.3132(6), Ni1–P8 2.4143(6), Ni2–P4 2.1983(8), Ni2–P5 2.2448(6), Ni2–P7 2.1811(7); P1–P3–P8 98.26(3), P3–P8–P6 97.79(3), P3–P1–P6 82.91(2), P3–P1–P4 84.04(3), P1–P4–P5 68.31(2), P4–P5–P3 104.92(4), P2–P4–P5 53.63(3), P4–P5–P2 55.29(3), P5–P2–P4 71.08(3), P5–P3–P8 95.97(3), P3–P8–P7 107.97(3), P6–P8–P7 79.88(3), P8–P7–P6 48.896(18), P7–P6–P8 51.23(2), P4–P1–P6 85.977(19), P1–P6–P7 96.32(2), P1–Ni1–P4 98.25(3), P3–Ni1–P5 56.10(2), P6–Ni1–P7 79.0(2), P8–Ni1–P7 59.00(2).

large P4–P5 distance of 2.5499(9) Å. In addition, this unit is connected to a second P₃ ring (P6, P7 and P8) via a P–P single bond (P3–P7 2.1702(8) Å). The P₈ framework is stabilised by two LSi moieties. Each silicon atom is connected to two phosphorus atoms. The whole framework is capped by a [(IDipp)Ni] fragment connected to three P atoms (P4, P5 and P7) (Fig. 3).

The Ni1–Ni2 distance (2.4126(4) Å) also deserves to be commented on. This value is consistent with an estimated value of 2.48 Å derived from the covalent radius of a single nickel atom (1.24 Å).²¹ While covalent metal–metal bonds are common for nickel(i) complexes,²² only a few related dinickel(0) complexes have been described with Ni⁰–Ni⁰ distances ranging from 2.437 to 2.572 Å.²³ A notable example is the isonitrile complex [Ni₂(μ-CNMe)(CNMe)₂(μ-PPH₂CH₂PPH₂)₂] reported by Kubiak and co-workers with a Ni–Ni separation of 2.572(1) Å.^{23a}

In order to investigate the bonding situation in more detail, the electronic structure was analysed by calculating intrinsic bond orbitals (IBOs)²⁴ at the PBE/def2-TZVP level of theory. A truncated model of **3'** (with iPr of **3** replaced by Me groups) was used for the calculations. The composition of the IBOs suggests a 3d¹⁰ configuration for the two Ni atoms. Seven two-centre-two-electron P–P bonds, four doubly occupied IBOs involving the Si–P bonds and, additionally, three three-centre-two-electron bonds were calculated. One of the multicentre bonds (see Fig. S35, ESI†) suggests a Ni1–Ni2 interaction. The presence of a weak Ni–Ni bond is also supported by the calculated Mayer bond order of 0.3. The short Ni1–Ni2 distance might thus mainly be explained by the constrained alignment of the core of the cluster and additional significant contributions of the multicentre bonds.

Multinuclear NMR spectra of **3** suggest the presence of two isomers in solution in an approximate ratio of 3:1 due to the asymmetric L ligand. It is worth noting a similar ratio was found in the solid state, in the disorder of the diketimate ligand (L) backbone (see Fig. S29, ESI†). As a result, the ¹H, ¹³C NMR spectra are complex, but confirm the presence of all molecular components. The ²⁹Si NMR spectrum shows two broad resonances at δ = –3.9 ppm and 60.8 ppm. However, the ³¹P{¹H} NMR spectrum is particularly informative, showing two ABCDEMSX spin systems independent of temperature (see Fig. 4, Fig. S23 and S24, ESI†). To aid in assigning the signals, ³¹P and ²⁹Si NMR chemical shieldings were calculated for the main isomer (see Tables S3 and S4, ESI†) of the slightly

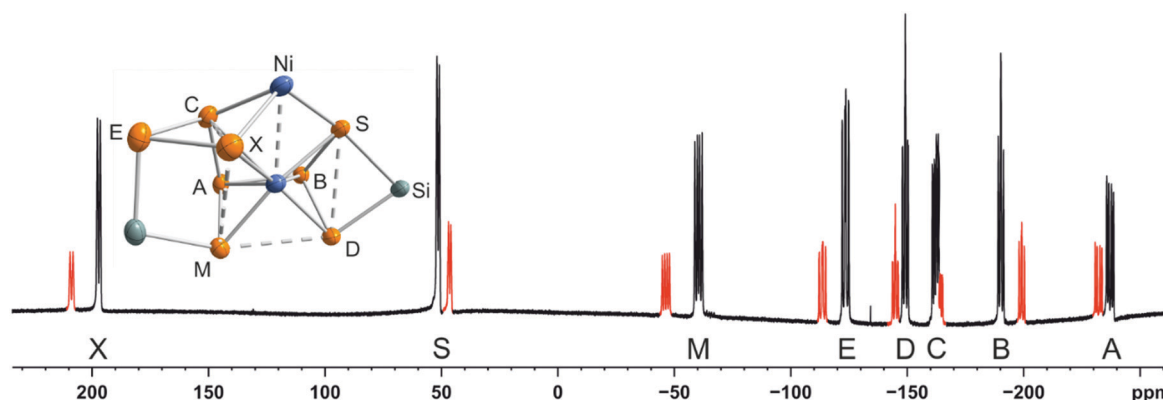


Fig. 4 ³¹P{¹H} NMR spectrum of cluster **3** in C₆D₆ at room temperature with nuclei assigned to the ABCDEMSX spin system; two isomers are present in solution (signals colour-coded in black and red, assigned based on integration); chemical shifts for isomer A: δ/ppm = –237.1 (P_A), –190.3 (P_B), –162.2 (P_C), –149.2 (P_D), –123.5 (P_E), –60.5 (P_M), 51.3 (P_S), 191.1 (P_X); isomer B: δ/ppm –232.2 (P_A), –199.3 (P_B), –164.8 (P_C), –145.0 (P_D), –113.7 (P_E), –46.5 (P_M), 46.4 (P_S), 208.8 (P_X); DFT-calculated and simulated coupling constants are presented in the ESI† (see Table S1); insets: representation of the core of the cluster; thermal ellipsoids are drawn at the 40% probability level.



truncated model cluster 3' at the TPSS/pcSseg-2 level of theory. Complex 2 was chosen as a reference system and the resonances of the $^{31}\text{P}\{^1\text{H}\}$ NMR spectrum (Fig. 4) were assigned according to the calculation, allowing for the iterative fitting of the $^{31}\text{P}\{^1\text{H}\}$ NMR spectrum of 3 (see the ESI†). DFT-calculated $J(^{31}\text{P}, ^{31}\text{P})$ coupling constants were used as an initial starting point for the fitting procedure (see Table S1, ESI†). Five large $^1J(^{31}\text{P}, ^{31}\text{P})$ coupling constants (-204.2 to -409.7 Hz) and one unexpectedly small $^1J(^{31}\text{P}, ^{31}\text{P})$ coupling constant of -7.5 Hz between nuclei P_A and P_B were derived. The small $^1J(\text{P}_\text{A}, \text{P}_\text{B})$ (-7.5 Hz) coupling constant might be explained by the relatively long distance of the nuclei P_A and P_B observed by X-ray crystallography (P3-P8 2.4018(7) Å). Notably, a rather large coupling constant of 218.1 Hz between nuclei P_D and P_M is observed despite the long P–P distance ($\text{P1} \cdots \text{P6}$ 3.0176(7) Å) deduced from the solid-state structure. We reason this finding as a through space coupling as observed also in other polyphosphorus compounds.²⁵

In summary, we have shown that the (NHC)Ni synthon $[(\text{NHC})\text{Ni}(\eta^2\text{-vtms})_2]$ ($\text{NHC} = \text{IDipp}$, IMes , $\text{vtms} = \text{Me}_3\text{SiCH}=\text{CH}_2$) effects a unusual dimerisation of $[\text{LSi}(\eta^2\text{-P}_4)]$ to form the $\text{Ni}_2\text{Si}_2\text{P}_8$ cluster 3. Additionally, the classical (NHC)Ni complexes 1a, b and 2 have been isolated alongside. Such Ni complexes show great potential as starting materials for the synthesis of ternary phosphorus cluster such as compound 3 as they are well-defined and conveniently prepared. Derivatisation reactions of the cluster core 3 through the substitution of the diketiminate ligands L may further enhance the diversity of this class of cluster molecules. An extension of the synthetic methodology reported here and the use of 3 and related clusters as single source precursors for phosphorus-based materials will be of significant future interest.

We thank Dr Peter Coburger for assistance with the DFT calculations and Julia Leitl for help with preparing the manuscript. Generous financial support by the Deutsche Forschungsgemeinschaft (WE4621/3-1 and WO1496/7-1), the European Research Council (CoG 772299) and the Fonds der Chemischen Industrie (Kekulé fellowship to G.H.) is gratefully acknowledged.

Conflicts of interest

There are no conflicts to declare.

Notes and references

- 1 V. Jourdain, E. T. Simpson, M. Paillet, T. Kasama, R. E. Dunin-Borkowski, P. Poncharal, A. Zahab, A. Loiseau, J. Robertson and P. Bernier, *J. Phys. Chem. B*, 2006, **110**, 9759.
- 2 (a) H. Li, G. Li and Z. Liu, *ACS Omega*, 2019, **4**, 2075; (b) A. Parra-Puerto, K. L. Ng, K. Fahy, A. E. Goode, M. P. Ryan and A. Kucernak, *ACS Catal.*, 2019, **9**, 11515; (c) Z. Sun, M. Zhu, M. Fujitsuka, A. Wang, C. Shi and T. Majima, *ACS Appl. Mater. Interfaces*, 2017, **9**, 30583; (d) Y. Shi and B. Zhang, *Chem. Soc. Rev.*, 2016, **45**, 1529.
- 3 G. Zhang, G. Wang, Y. Liu, H. Liu, J. Qu and J. Li, *J. Am. Chem. Soc.*, 2016, **138**, 14686.
- 4 (a) S. T. Oyama, T. Gott, H. Zhao and Y.-K. Lee, *Catal. Today*, 2009, **143**, 94; (b) I. I. Abu and K. J. Smith, *Appl. Catal., A*, 2007, **328**, 58; (c) S. Yang, C. Liang and R. Prins, *J. Catal.*, 2006, **237**, 118; (d) Y. Shu and S. T. Oyama, *Chem. Commun.*, 2005, 1143; (e) S. T. Oyama, *J. Catal.*, 2003, **216**, 343; (f) R. Prins, G. Pirngruber and T. Weber, *Chimia*, 2001, **55**, 791.
- 5 S. L. Brock, S. C. Perera and K. L. Stamm, *Chem. – Eur. J.*, 2004, **10**, 3364.
- 6 (a) Z. Jin, P. Li, X. Huang, G. Zeng, Y. Jin, B. Zheng and D. Xiao, *J. Mater. Chem. A*, 2014, **2**, 18593–18599; (b) Y. Li, X. Jiang, Z. Miao, J. Tang, Q. Zheng, F. Xie and D. Lin, *ChemCatChem*, 2019, **12**, 917–925; (c) H.-W. Man, C.-S. Tsang, M. Meng-Jung Li, J. Mo, B. Huang, L. Yoon Suk Lee, Y.-C. Leung, K.-Y. Wong and S. Chi Edman Tsang, *Appl. Catal., B*, 2019, **242**, 186–193; (d) S. Anantharaj, S. Rao Ede, K. Sakthikumar, K. Karthick, S. Mishra and S. Kundu, *ACS Catal.*, 2016, **6**(12), 8069–8097.
- 7 J. Chang, K. Li, Z. Wu, J. Ge, C. Liu and W. Xing, *ACS Appl. Mater. Interfaces*, 2018, **10**, 26303–26311.
- 8 M. Shatruk, in *Fundamentals and applications of phosphorus nano-materials*, ed. H.-F. Ji, American Chemical Society, Washington, DC, 2019, vol. 6, pp. 103–134.
- 9 (a) K. L. Stamm, J. C. Garno, G.-y. Liu and S. L. Brock, *J. Am. Chem. Soc.*, 2003, **125**, 4038; (b) S. C. Perera, G. Tsoi, L. E. Wenger and S. L. Brock, *J. Am. Chem. Soc.*, 2003, **125**, 13960.
- 10 S. Carenco, I. Resa, X. Le Goff, P. Le Floch and N. Mézailles, *Chem. Commun.*, 2008, 2568.
- 11 (a) A. E. Henkes, Y. Vasquez and R. E. Schaak, *J. Am. Chem. Soc.*, 2007, **129**, 1896; (b) R.-K. Chiang and R.-T. Chiang, *Inorg. Chem.*, 2007, **46**, 369.
- 12 (a) T. Grell, D. M. Yufanyi, A. K. Adhikari, M.-B. Sárosi, P. Lönnecke and E. Hey-Hawkins, *Pure Appl. Chem.*, 2019, **91**, 103; (b) A. Kircali Akdag, P. Lönnecke and E. Hey-Hawkins, *Z. Anorg. Allg. Chem.*, 2014, **640**, 271.
- 13 P. Dapporto, S. Midollini and L. Sacconi, *Angew. Chem., Int. Ed. Engl.*, 1979, **18**, 469.
- 14 Selected examples of P_4 activation using Ni^{II} sources: (a) M. Di Vaira, S. Midollini and L. Sacconi, *J. Am. Chem. Soc.*, 1979, **101**, 1757; (b) M. Di Vaira, C. A. Ghilardi, S. Midollini and L. Sacconi, *J. Am. Chem. Soc.*, 1978, **100**, 2550.
- 15 Selected examples of P_4 activation using Ni^{I} sources: (a) S. Pelties, D. Herrmann, B. d. Bruin, F. Hartl and R. Wolf, *Chem. Commun.*, 2014, **50**, 7014; (b) S. Yao, Y. Xiong, C. Milsman, E. Bill, S. Pffirmann, C. Limberg and M. Driess, *Chem. – Eur. J.*, 2010, **16**, 436; (c) O. J. Scherer, J. Braun, P. Walther and G. Wolmershäuser, *Chem. Ber.*, 1992, **125**, 2661; (d) O. J. Scherer, J. Braun and G. Wolmershäuser, *Chem. Ber.*, 1990, **123**, 471; (e) O. J. Scherer, T. Dave, J. Braun and G. Wolmershäuser, *J. Organomet. Chem.*, 1988, **350**, C20–C24.
- 16 B. Zarzycki, T. Zell, D. Schmidt and U. Radius, *Eur. J. Inorg. Chem.*, 2013, 2051.
- 17 G. Hierlmeier, P. Coburger, N. P. van Leest, B. de Bruin and R. Wolf, *Angew. Chem., Int. Ed.*, 2020, **59**, 14148–14153.
- 18 Y. Xiong, S. Yao, E. Bill and M. Driess, *Inorg. Chem.*, 2009, **48**, 7522.
- 19 Y. Xiong, S. Yao, M. Brym and M. Driess, *Angew. Chem., Int. Ed.*, 2007, **46**, 4511.
- 20 (a) M. R. Elsby, J. Liu, S. Zhu, L. Hu, G. Huang and S. A. Johnson, *Organometallics*, 2019, **38**, 436; (b) M. R. Elsby and S. A. Johnson, *J. Am. Chem. Soc.*, 2017, **139**, 9401.
- 21 B. Cordero, V. Gómez, A. E. Platero-Prats, M. Revés, J. Echeverría, E. Cremades, F. Barragán and S. Alvarez, *Dalton Trans.*, 2008, 2832.
- 22 J.-C. Hierso, *Chem. Rev.*, 2014, **114**, 4838.
- 23 (a) D. L. DeLaet, P. E. Fanwick and C. P. Kubiak, *Organometallics*, 1986, **5**, 1807; (b) A. Kempter, C. Gemel, T. Cadenbach and R. A. Fischer, *Organometallics*, 2007, **26**, 4257; (c) O. Serrano, E. Hoppe, J. C. Fettingier and P. P. Power, *J. Organomet. Chem.*, 2011, **696**, 2217; (d) A. Seifert and G. Linti, *Inorg. Chem.*, 2008, **47**, 11398.
- 24 G. Knizia, *J. Chem. Theory Comput.*, 2013, **9**, 4834.
- 25 For representative examples, see: (a) C. Taube, K. Schwedtmann, M. Noikham, E. Somsook, F. Hennesdorf, R. Wolf and J. J. Weigand, *Angew. Chem., Int. Ed.*, 2020, **59**, 3585; (b) P. Coburger, P. Bielytskiy, D. Williamson, E. Rys, A. Kreienbrink, P. Lönnecke, J. Matysik and E. Hey-Hawkins, *Chem. – Eur. J.*, 2019, **25**, 11456; (c) H. C. E. McFarlane and W. McFarlane, *Polyhedron*, 1999, **18**, 2117; (d) H. C. E. McFarlane and W. McFarlane, *Polyhedron*, 1988, **7**, 1875.

